MVA2007 IAPR Conference on Machine Vision Applications, May 16-18, 2007, Tokyo, JAPAN

A case study of higher order Tikhonov regularization terms influence on the convergence of active contours

Moqing Zhang and Patrice Delmas

Department of Computer Science, Tamaki Campus, the University of Auckland.
Email: patrice@cs.auckland.ac.nz

Abstract

An explicit snake is a smooth closed curve which deforms towards the desired features in an image. There are two types of force controlling the motion of the snake: internal and external forces. The former usually constrains the snake's curvature and tension, through first and second Tikhonov smoothness force terms, while the latter generates attraction forces. To investigate the possible role of higher Tikhonov constraint parameters, third and fourth force regularizing terms are added in this study. The related theoretical equations are derived and the respective influence of the four internal force terms are examined and followed on test images. While still at the preliminary stage, the present study shows that the added internal force terms may improve the smoothness and convergence of the snake.

1 Introduction

An explicit snake model provides a unified solution to a set of visual problems which were treated in different ways in the past. In this model, edges, lines and regions contours can be extracted by the same mechanisms and as such is a powerful tool for high-level image processing.

The first active contour, also called snake for its characteristic motion over time, was proposed by Kass, Witkin and Terzopulos[1] in the late 1980's. Since then a significant number of studies has been conducted to improve its behaviour and resolve the problems related to its optimal convergence. Cohen's[2] balloon model is an additional force which makes the snake inflate or deflate. The Gradient Vector Flow model proposed by Chenyang and Prince[3] computes the external force as a diffusion of the gradient vectors of a gray-level or binary edge map derived from the image thus allowing convergence towards concave objects. In 1993, Cohen L.D. and Cohen I.[4] suggested using Chamfer distance to edge points as external force. The basic ideas of these solutions are to increase the capture range of the external force, so that the initial snakes do not necessarily lie very close to the regions of interests.

Almost all of the existing explicit snake models have the same internal force which is composed of the first and second Tikhonov smooth force terms. Higher order Tikhonov smoothness force terms could also have some effects on the snake internal constraints dynamic behaviour but this has never been investigated. Incidentally, Tikhonov demonstrated that the minimisation of ill-posed problems (such as extracting object contours from an edge map) regularized by an infinite sum of Tikhonov smoothing terms, of increasing order, could lead to an optimal solution [5]. A first step towards exploring these possible effects is the addition of third and fourth order Tikhonov smoothing terms to the snake internal constraint. After a theoretical characterisation of these added terms, the roles of the internal force terms are examined.

2 Explicit snake

2.1 Model

An explicit snake (parametric snake) is a specific type of deformable model, which is a mapping:

$$\Omega = [0,1] \rightarrow R^2$$
$$s \mapsto v(s) = (x(s), y(s))$$

Where s denotes the curvilinear abscissa and (x,y) the Cartesian coordinates of the snake points. An explicit snake model is defined as a space of admissible deformations A and a functional E to minimize. This functional represents the energy of the model which will be minimized and has the following form:

$$E : A \rightarrow R$$

$$v \mapsto E_{snake}(v) = \int_0^1 E_{snake}(v(s))ds$$
$$= \int_0^1 E_{\text{int}}(v(s)) + E_{ext}(v(s))ds \qquad (1)$$

where

$$E_{\text{int}} = \alpha(s)|v_s(s)|^2 + \beta(s)|v_{ss}(s)|^2 + T(s)|v_{sss}(s)|^2 + F(s)|v_{ssss}(s)|^2 \qquad (2)$$

$$E_{ext} = E_{image}(v(s)) + E_{constrain}(v(s))$$

Assume v is a local minimum for E, equation (1) leads to the following associated Euler-Lagrange equation:

$$-(\alpha v_s)_s + (\beta v_{ss})_{ss} - (T v_{sss})_{sss} + (F v_{ssss})_{ssss} + \nabla E_{image}(v) + \nabla E_{constrain}(v) = 0 \quad (3)$$

$(v(0), v_s(0), v(1)$ and $v_{ss}(1)$ are known.)

Here,$v_s(s)$, $v_{ss}(s)$, $v_{sss}(s)$ and $v_{ssss}(s)$ denote derivatives of $v(s)$, $\alpha(s)$, $\beta(s)$, $T(s)$ and $F(s)$ are the weights of $v_s(s)$, $v_{ss}(s)$, $v_{sss}(s)$ and $v_{ssss}(s)$ respectively, one can control the importance of $v_s(s)$, $v_{ss}(s)$, $v_{sss}(s)$ and $v_{ssss}(s)$ by adjusting the weights $\alpha(s)$, $\beta(s)$, $T(s)$ and $F(s)$. E_{image} refers to the image energy which correspond to the desired attributes and $E_{constrain}$ is the external constraint force. In practice, we always give a weight to the image force and external force respectively, thus equation (3) becomes:

$$-(\alpha v_s)_s + (\beta v_{ss})_{ss} - (T v_{sss})_{sss} + (F v_{ssss})_{ssss} + \kappa \nabla E_{image}(v) + \kappa_p \nabla E_{constrain}(v) = 0 \quad (4)$$

A solution can be seen either as realizing the equilibrium of the forces in the equation (4) or reaching the minimum of the energy (1).

2.2 Numerical solution

Assume $f(v) = \kappa \nabla E_{image}(v) + \kappa_p \nabla E_{constrain}(v)$, then (4) becomes:

$$-(\alpha v_s)_s + (\beta v_{ss})_{ss} - (T v_{sss})_{sss} + (F v_{ssss})_{ssss} + f(v) = 0 \quad (5)$$

Using the finite difference method approximate the derivatives of v, assume the special distance is equal to 1 constantly, then the left terms of (5) can be expressed as:

$$\begin{aligned}(\alpha v_s)_s &= +\alpha_{i+1}(v_{i+1} - v_i) - \alpha_i(v_i - v_{i-1}) \\ &= +\alpha(v_{i+1} - 2v_i + v_{i-1}) \text{ for } \alpha \text{ constant}\end{aligned}$$

$$\begin{aligned}(\beta v_{ss})_{ss} &= +\beta_{i+1}(v_{i+2} + v_i - 2v_{i+1}) \\ &\quad -2\beta_i(v_{i+1} + v_{i-1} - 2v_i) \\ &\quad +\beta_{i-1}(v_{i-2} + v_i - 2v_{i-1}) \\ &= +\beta(v_{i-2} - 4v_{i-1} + 6v_i - 4v_{i+1} + v_{i+2}) \\ &\quad \text{for } \beta \text{ constant}\end{aligned}$$

$$\begin{aligned}(T v_{sss})_{sss} &= +T_{i+2}(v_{i+3} - 3v_{i+2} + 3v_{i+1} - v_i) \\ &\quad -3T_{i+1}(v_{i+2} - 3v_{i+1} + 3v_i - v_{i-1}) \\ &\quad +3T_i(v_{i+1} - 3v_i + 3v_{i-1} - v_{i-2}) \\ &\quad -T_{i-1}(v_i - 3v_{i-1} + 3v_{i-2} - v_{i-3}) \\ &= T(v_{i-3} - 6v_{i-2} + 15v_{i-1} - 20v_i \\ &\quad +15v_{i+1} - 6v_{i+2} + v_{i+3}) \\ &\quad \text{for } T \text{ constant}\end{aligned}$$

$$\begin{aligned}(F v_{ssss})_{ssss} &= +F_{i+2}(v_{i+4} - 4v_{i+3} + 6v_{i+2} - 4v_{i+1} + v_i) \\ &\quad -4F_{i+1}(v_{i+3} - 4v_{i+2} + 6v_{i+1} - 4v_i + v_{i-1}) \\ &\quad +6F_i(v_{i+2} - 4v_{i+1} + 6v_i - 4v_{i-1} + v_{i-2}) \\ &\quad -4F_{i-1}(v_{i+1} - 4v_i + 6v_{i-1} - 4v_{i-2} + v_{i-3}) \\ &\quad +F_{i-2}(v_i - 4v_{i-1} + 6v_{i-2} - 4v_{i-3} + v_{i-4}) \\ &= F(v_{i-4} - 8v_{i-3} + 28v_{i-2} - 56v_{i-1} + 70v_i \\ &\quad -56v_{i+1} + 28v_{i+2} - 8v_{i+3} + v_{i+4}) \\ &\quad \text{for } F \text{ constant}\end{aligned}$$

Thus (5) can be written in matrix form:

$$AV + f = 0$$

Where A is a quasi nona-diagonal circulant Toepliz matrix:

$$A = \begin{pmatrix}
a_5 & a_4 & a_3 & a_2 & a_1 & 0 & 0 & \cdots & 0 & a_9 & a_8 & a_7 & a_6 \\
a_6 & a_5 & a_4 & a_3 & a_2 & a_1 & 0 & \cdots & 0 & 0 & a_9 & a_8 & a_7 \\
a_7 & \cdots & a_5 & a_4 & a_3 & a_2 & a_1 & \cdots & 0 & 0 & 0 & a_9 & a_8 \\
a_8 & \cdots & \cdots & a_5 & a_4 & a_3 & a_2 & \cdots & 0 & 0 & 0 & 0 & a_9 \\
a_9 & a_8 & \cdots & \cdots & a_5 & a_4 & a_3 & \cdots & 0 & 0 & 0 & 0 & 0 \\
0 & a_9 & a_8 & \cdots & \cdots & a_5 & a_4 & \cdots & 0 & 0 & 0 & 0 & 0 \\
0 & 0 & a_9 & a_8 & \cdots & \cdots & a_5 & \cdots & 0 & 0 & 0 & 0 & 0 \\
0 & 0 & 0 & a_9 & a_8 & a_7 & a_6 & a_5 & a_4 & a_3 & a_2 & a_1 & 0 \\
0 & \cdots & \cdots & 0 & a_9 & a_8 & \cdots & \cdots & \cdots & \cdots & \cdots & a_2 & a_1 \\
0 & \cdots & \cdots & \cdots & 0 & a_9 & a_8 & a_7 & a_6 & a_5 & a_4 & a_3 & a_2 \\
\vdots & & & & \vdots & & & & \vdots & & & \vdots & \\
\vdots & & & & \vdots & & & & \vdots & & & \vdots & \\
a_1 & 0 & \cdots & \cdots & \cdots & 0 & a_9 & a_8 & a_7 & a_6 & a_5 & a_4 & a_3 \\
a_2 & a_1 & 0 & \cdots & \cdots & \cdots & 0 & a_9 & \cdots & \cdots & \cdots & \cdots & a_3 \\
a_3 & a_2 & a_1 & 0 & \cdots & \cdots & \cdots & 0 & a_9 & \cdots & \cdots & \cdots & a_4 \\
a_4 & a_3 & a_2 & a_1 & 0 & \cdots & \cdots & \cdots & 0 & a_9 & a_8 & a_7 & a_6 & a_5
\end{pmatrix}$$

The nine a_i weights are derived from the above equations:

$$a = \begin{pmatrix} F \\ -T - 8F \\ \beta + 6T + 28F \\ -\alpha - 4\beta - 15T - 56F \\ 2\alpha + 6\beta + 20T + 70F \\ -\alpha - 4\beta - 15T - 56F \\ \beta + 6T + 28F \\ -T - 8F \\ F \end{pmatrix}$$

V and f denote the vector of the locii and forces of the snake points.

As explained in[1], to solve equation 5, the right-hand side of the equation is set equal to the product of a time step size and the negative time derivatives of the left-hand sides. For simplicity, assume f is constant during a time step, leading to an explicit Euler method with respect to the external force. Because the matrix A completely specified the internal forces, we can evaluate the time derivative at time t rather than time t-1 and consequently arrive

at an implicit Euler step for the internal forces. The resulting equation is:

$$AV_t + f_{t-1} = -\gamma(V_t - V_{t-1}) \qquad (6)$$

Equation (6) can be solved by matrix inversion:

$$V_t = (A + \gamma I)^{-1}(V_{t-1} - f_{t-1}) \qquad (7)$$

Note that the matrix of equation (7) needs to be inverted once if the smoothness parameters are set constant through the snake temporal evolution. This can be achieved via a LU decomposition scheme in $O(n)$ time [6],[7] or through the direct computation of its coefficients [8].

3 Experimental tests

In equation (4) each term appears as a force applied to the snake. The first four terms are the internal forces namely the first, second, third and fourth order Tikhonov smoothness force terms where $\alpha(s)$, $\beta(s)$, $T(s)$ and $F(s)$ are their associated weights.

In order to examine the influence of the high order smoothness parameters, two groups of experiments are conducted, using different images, different distances between the snake discrete points. The first group use a 64*64 U shape binary image [9], the snake is manually initialized as a square around the desired feature, the distance between the snake points is set to 2, the weight of the image force is set to 1. Another group uses a 128*128 synthetic lip colour image, manual initialization, the distance between the snake points is set to 3, the weight of the image force is set to 0.5;. In both group, the time step is set to 1 and the image force is adapted from the GVF model.
The parameters used in both group are shown in Table 1 and Table 2 respectively. Note that a study of each parameter's separate influence, over an order of magnitude, on the active contour convergence was conducted beforehand but cannot be described here for lack of space.

The first two images of Figure1 show the snake convergence using only α and β coefficients. The snake almost converges towards the deep concave regions of the U-shape.

Once the third term is added, the final snake convergence towards the concave region is improved, as shown in the last two images of Figure1.

From the first two images of Figure2, it can be seen that the fourth order smoothing term can play a similar role as the third term did previously. The last two images of Figure2 shows that the third

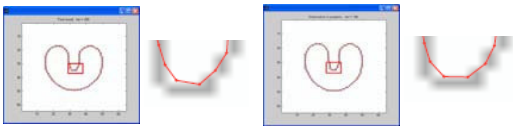

Figure 1: Leftmost: final snake using the parameters in the first row of Table 1; next: zoom in of the concave area; next: final snake using the parameters in the second row of Table 1; rightmost: zoom in of the concave area.

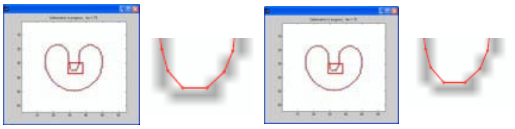

Figure 2: Leftmost: final snake with the parameters in the third row of Table 1; next: zoom in of the concave area; next: final snake using the parameters in the fourth row of Table 1; rightmost: zoom in of the concave area.

and fourth order smoothing applied together may achieve a better convergence.

The results corresponding to the parameters listed in Table 2 are shown in Figure 3. Two sections of the critical area of lip contours are zoomed in right column. One is the lower part of the Cupidon arch (up cell), the other is the mouth left corner (bottom cell).

According to the topology of the lip image, the extracted contour should be symmetric, the line between the two middle points of the final snake should be parallel to the image edge; Regarding the left corner of the lip, because it links the upper and lower lips, the snake in this area should be smoothed. It can be seen in Figure 3 that the active contour achieves a better convergence when the higher smoothness terms are added.

From the experiments in this group, it can be observed that the third and fourth order parameters can help achieve a convergence closer to the desired feature. Weights T and F may control micro adjustment of the smoothness and convergence.

4 Conclusion

We have seen that the four smoothing terms control the snake in different way: the first order term imposes the elasticity to the snake, all the others including the second, the third and the fourth order terms impose the curvatureness of the snake. Because the third and the fourth order terms may provide micro-adjustment of the curvature control they may play an important role in optimal convergence of the active contour. However they do incur

Table 1: Parameters used in the group using the U shape binary image.

1	$\alpha = 0.01, \beta = 0.1, T = 0, F = 0, iter = 250$
2	$\alpha = 0.01, \beta = 0.1, T = 0.5, F = 0, iter = 250$
3	$\alpha = 0.01, \beta = 0.1, T = 0, F = 1, iter = 75$
4	$\alpha = 0.01, \beta = 0.1, T = 0.1, F = 1, iter = 75$

Table 2: Parameters used in the group using the lip image.

1	$\alpha = 0.1, \beta = 0, T = 0, F = 0, iter = 250$
2	$\alpha = 0.1, \beta = 0.2, T = 0, F = 0, iter = 250$
3	$\alpha = 0.1, \beta = 0.2, T = 1, F =, iter = 75$
4	$\alpha = 0.1, \beta = 0.2, T = 1, F = 1, iter = 75$

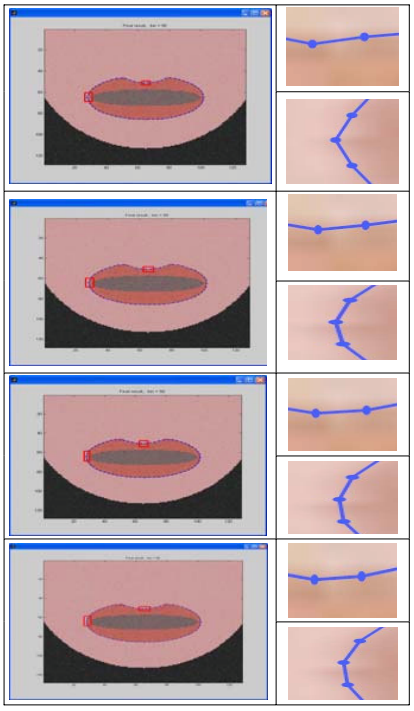

Figure 3: Left: Snake convergence results using the parameters in the corresponding rows of Table 2; Right: top: the magnified Cupidon arch region; bottom: the magnified left corner area of the lip.

more complex stiffness matrix computation hence slowing down slightly the convergence process.

The present study has some implications. Theoretically a variety of higher order Tikhonov smooth terms could be developed to improve the snake control. In practice various internal forces could be chosen to improve the convergence depending on the topology of the desired feature and the image features characteristics. We are currently conducting studies to derive an optimal selection of Tikhonov smoothing terms weights on test images.

References

[1] M. Kass, A. Witkin, and D. Terzopoulos, "Snakes: active contour models," *International Journal of Computer Vision*, vol. 1, no. 4, pp. 321–331, 1987.

[2] L. D. Cohen, "On active contour models and balloons," *CVGIP: Image Understanding*, vol. 53, no. 2, pp. 211–218, 1991.

[3] C. Xu and J. Prince, "Snakes, shapes and gradient vector flow," *IEEE Transactions on Image Processing*, vol. 7, no. 3, pp. 359–369, 1998.

[4] L. D. Cohen and I. Cohen, "Finite-element methods for active contour models and balloons for 2-d and 3-d images," *Pattern Analysis and Machine Intelligence.IEEE Transactions*, vol. 15, no. 11, pp. 1131–1147, 1993.

[5] A. Tikhonov and V. Arsenine, *Méthodes de résolution de problèmes mal posés*. MIR, 1974.

[6] I. Gladwell and R. Wait, eds., *A survey of numerical methods for partial differential equations*. Clarendon: Oxford, 1979.

[7] A. Benson and D. Evans, "Mathematical software," *ACM TRANS*, vol. 3, pp. 96–103, 1977.

[8] P. Delmas, N. Eveno, and P. Y. Coulon, "Towards automatic lip tracking," (Dunedin), Proceedings of the Image and Vision Computing New Zealand Conference, 26-28 November 2001.

[9] C. Xu and J. L. Prince, "Gvf snake demo." http://iacl.ece.jhu.edu/projects/gvf/snakedemo/, visited on 1/7/2006.